Title

ATP Hydrolysis by the SNF2 Domain of Dnmt5 Is Coupled to Both Specific Recognition and Modification of Hemimethylated DNA

Journal

Molecular Cell, 79(1)

ISSN

1097-2765

Authors

Dumesic, Phillip A
Stoddard, Caitlin I
Catania, Sandra
et al.

Publication Date

2020-07-01

DOI

10.1016/j.molcel.2020.04.029

Peer reviewed

HHS Public Access

Author manuscript

Mol Cell. Author manuscript; available in PMC 2021 July 02.

Published in final edited form as:

Mol Cell. 2020 July 02; 79(1): 127–139.e4. doi:10.1016/j.molcel.2020.04.029.

ATP hydrolysis by the SNF2 domain of Dnmt5 is coupled to both specific recognition and modification of hemimethylated DNA

Phillip A. Dumesic[1], **Caitlin I. Stoddard**[1], **Sandra Catania**[1], **Geeta J. Narlikar**[1,*], **Hiten D. Madhani**[1,2,3,*]

[1]Department of Biochemistry and Biophysics, University of California, San Francisco, CA 94158, USA

[2]Chan-Zuckerberg Biohub, San Francisco, CA 94158, USA

[3]Lead Contact

SUMMARY

C. neoformans Dnmt5 is an unusually specific maintenance-type CpG methyltransferase (DNMT) that mediates long-term epigenome evolution. It harbors a DNMT domain and SNF2 ATPase domain. We find that the SNF2 domain couples substrate specificity to an ATPase step essential for DNA methylation. Coupling occurs independent of nucleosomes. Hemimethylated DNA preferentially stimulates ATPase activity, and mutating Dnmt5's ATP-binding pocket disproportionately reduces ATPase stimulation by hemimethylated versus unmethylated substrates. Engineered DNA substrates that stabilize a reaction intermediate by mimicking a 'flipped-out' conformation of the target cytosine bypass the SNF2 domain's requirement for hemimethylation. This result implies that ATP hydrolysis by the SNF2 domain is coupled to the DNMT domain conformational changes induced by preferred substrates. These findings establish a new role for a SNF2 ATPase: controlling an adjoined enzymatic domain's substrate recognition and catalysis. We speculate that this coupling contributes to the exquisite specificity of Dnmt5 via mechanisms related to kinetic proofreading.

Graphical Abstract

*To whom correspondence should be addressed. hitenmadhani@gmail.com (H.D.M.); Geeta.Narlikar@ucsf.edu (G.J.N.).

AUTHOR CONTRIBUTIONS

P.A.D., C.I.S., G.J.N., and H.D.M. designed the study. P.A.D. and C.I.S. performed recombinant protein expression and purification. P.A.D. performed methyltransferase, ATPase, and EMSA assays. C.I.S. prepared nucleosomal substrates. S.C. generated *C. neoformans* strain. P.A.D., G.J.N., and H.D.M. wrote the manuscript. All authors contributed to editing the manuscript.

DECLARATION OF INTERESTS

The authors declare no competing interests.

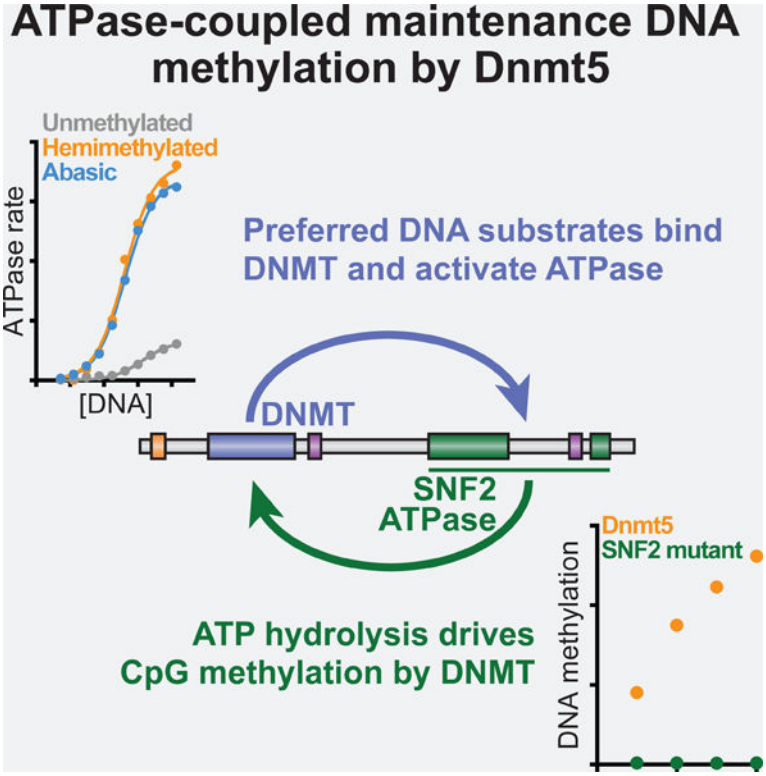

ETOC BLURB

Dumesic *et al.* discover coupling between the SNF2 ATPase and DNA methyltransferase domains of the CpG methyltransferase Dnmt5. Recognition of preferred substrates by the DNMT domain stimulates SNF2 domain ATP hydrolysis, which itself is required for DNA methyltransfer. ATPase coupling may underlie the exquisite specificity of Dnmt5's maintenance DNA methylation.

Keywords

DNA methylation; DNA methyltransferase; ATPase; Epigenetics; Dnmt5; Enzyme mechanism

INTRODUCTION

Methylation of the C5 position of cytosine (5mC) in eukaryotic genomes marks DNA sites in a potentially heritable manner. 5mC is present at repetitive elements and transposons, where it silences these elements for genome defense (Law and Jacobsen, 2010; Suzuki and Bird, 2008). Methylation is also found in the bodies of active genes, where its purpose is less clear (Feng et al., 2010; Huff and Zilberman, 2014; Schübeler, 2015; Zemach et al., 2010). In vertebrates, cytosine methylation is more widespread and occurs primarily at CG sites, both in gene bodies and intergenic regulatory regions. It is required for mammalian development, and can enforce long-term transcriptional repression of targeted genes, for instance during X chromosome inactivation, genomic imprinting, transposon suppression, and lineage-specific gene silencing (Jaenisch and Bird, 2003; Li et al., 1993; Smith and Meissner, 2013; Velasco et al., 2010).

An important aspect of cytosine methylation is its potential to enable the inheritance of gene silencing after loss of the initiating signal (Jones and Liang, 2009). In the simplest model, 5mC is maintained over cell divisions by a ‘maintenance’ DNA methyltransferase that acts preferentially on hemimethylated CG sites produced during DNA replication (Holliday and Pugh, 1975; Riggs, 1975). In contrast, an ‘establishment’ DNA methyltransferase deposits the initial 5mC mark de novo on an unmethylated CG template. Mammals encode DNA methyltransferases that broadly fall into these two classes. DNMT1 is widely expressed, is recruited to chromatin during DNA replication, and shows a kinetic preference for activity on hemimethylated as opposed to unmethylated substrates (Jeltsch and Jurkowska, 2016). In contrast, DNMT3A and DNMT3B exhibit equivalent activities on unmethylated and hemimethylated substrates, and are highly expressed in embryonic periods during which DNA methylation patterns are established.

Despite these general trends, high-resolution DNA methylation data have suggested that the segregation of roles between DNMT3A/B and DNMT1 might not be absolute: both enzyme classes appear to play a measurable role in DNA methylation establishment as well as maintenance (Arand et al., 2012; Jeltsch and Jurkowska, 2014; Jones and Liang, 2009; Riggs and Xiong, 2004). These results are consistent with the fact that the DNMT1 in vitro catalytic preference for hemimethylated sites is only 30–40-fold, seemingly insufficient for DNMT1 to preserve 5mC marks in a maintenance-only fashion, since this would require faithful replication of each of the 56 million CG sites in the human genome as either unmethylated or hemimethylated (Jeltsch, 2006; Jeltsch and Jurkowska, 2014). Therefore, ongoing de novo DNA methylation has been suggested to explain the stability of many 5mC marks. These findings highlight how the enzymological properties of an organism’s DNA methyltransferases might impose restrictions on how long the 5mC mark can be epigenetically inherited after loss of the mark’s initiating signal.

In this regard, our recent studies of the Dnmt5 family of eukaryotic cytosine methyltransferases are relevant. In this family—which is represented in fungi as well as in chlorophyte algae and stramenopiles—the DNMT domain is embedded in a multidomain architecture that includes a C-terminal SNF2 helicase-like domain (Iyer et al., 2011; Ponger and Li, 2005). Loss of function genomic studies revealed that Dnmt5 family methyltransferases are responsible for cytosine methylation at CG sites, and in some organisms represent the sole enzyme responsible for CG methylation (Huff and Zilberman, 2014). Our recent characterization of Dnmt5 in one such organism, the yeast *Cryptococcus neoformans*, revealed that the purified enzyme is an exquisitely specific maintenance-type methyltransferase in vitro, with no detectable de novo activity. Consistent with this observation, Dnmt5 was unable to restore 5mC landscapes when deleted from and subsequently reintroduced into a *C. neoformans* strain. Phylogenetic and functional analyses revealed that a species ancestral to *Cryptococcus* encoded a second DNA methyltransferase that possesses de novo methyltransferase activity (DnmtX), but this gene was lost 50–150 million years ago. Further work demonstrated that cytosine methylation has been maintained for millions of years since this loss through a process analogous to Darwinian evolution in which methylation persistence requires epigenetic inheritance, rare random 5mC losses and gains, and natural selection (Catania et al., 2020).

Here, we biochemically characterize *C. neoformans* Dnmt5 and uncover functional coupling between its SNF2 and DNMT domains that may contribute to its unusually high specificity for hemimethylated substrates. We find that ATP hydrolysis by the SNF2 domain is essential for DNA methyltransferase activity by the DNMT domain. Non-hydrolyzable nucleotide analogs perturb Dnmt5's affinity for DNA substrates and block DNA methylation activity. Strikingly, engineered DNA substrates predicted to stabilize the DNMT domain at intermediate steps of the cytosine methylation precatalytic pathway are sufficient to fully stimulate ATPase activity. These results demonstrate that SNF2-mediated ATP hydrolysis is both a response to recognition of a hemimethylated CG substrate and also itself required for productive substrate methylation. We discuss the possibility that these properties allow kinetic proofreading to enhance Dnmt5's specificity for its preferred substrates. More generally, these results reveal a previously undescribed role for a SNF2 ATPase in a DNA modification enzyme.

RESULTS

Dnmt5 is an ATP-dependent cytosine methyltransferase with high specificity for hemimethylated substrates

Dnmt5 proteins have unique architecture among DNA methyltransferase families: they contain a highly diverged DNMT domain followed by a RING domain, and a C-terminal region with SNF2 family homology (Huff and Zilberman, 2014; Iyer et al., 2011; Ponger and Li, 2005) (Figure 1A). Dnmt5 orthologs mediate CG methylation in diverse eukaryotes, including the yeast *C. neoformans*, where Dnmt5 is the organism's sole DNA methyltransferase. Initial characterization of Dnmt5 in this system revealed that it has a strong in vivo and in vitro preference for action on hemimethylated, but not unmethylated, DNA substrates, and that it requires ATP addition to the reaction (Catania et al., 2020). The unusual specificity profile of this enzyme motivated us to examine the regulation of its activity in vitro, and to interrogate the role of its SNF2 domain.

We expressed the *C. neoformans* Dnmt5 protein in *S. cerevisiae* and isolated it to >90% purity (Figure S1A). Its DNA methyltransferase activity was tested under multiple turnover conditions using 60 bp dsDNA substrates whose three CG motifs were uniformly unmethylated, hemimethylated, or symmetrically methylated (Figure 1B). Confirming our prior results, in the absence of ATP, no activity was observed on any substrate. When ATP was added, activity was observed on hemimethylated substrates but not on unmethylated or symmetrically methylated substrates (Figure 1C). The rate of methylation was comparable to that of the well-studied maintenance methyltransferase DNMT1 (Pradhan et al., 1999) (Figure 1D). Importantly, when Dnmt5 was expressed and purified from its native host *C. neoformans* instead of from the orthologous system *S. cerevisiae*, protein yields were substantially lower, but the enzyme exhibited comparable qualitative and quantitative properties, confirming that its observed substrate preferences and ATP dependence were not an artifact of its expression system (Figure S1A–D).

Given its lack of activity on unmethylated DNA substrates, we tested Dnmt5 under conditions that might provoke a latent de novo methyltransferase activity. First, since the Dnmt5 chromodomain has been shown to recognize trimethylation of histone H3 at lysine 9

(Catania et al., 2020), we tested Dnmt5 activity in the presence of peptides corresponding to the histone H3 N-terminal tail, with or without K9 trimethylation. When saturating concentrations of either peptide were present, reaction rates on hemimethylated substrates were comparable, and activity remained undetectable on unmethylated DNA (Figure 1E). Second, since DNMT1 activity on unmethylated CG motifs can be stimulated by nearby methylation marks (Tollefsbol and Hutchison, 1997), we tested whether the addition of unmethylated CG sites would increase Dnmt5's methylation of a DNA substrate containing a single hemimethylated CG site (Figure S1E,F). Such a result would indicate unveiled de novo activity. In fact, addition of these unmethylated CG sites did not affect Dnmt5's initial methylation rate, nor did it affect the endpoint quantity of methyl marks that were deposited (at 4 hr—a timepoint at which the methylation reaction was empirically found to have ceased, perhaps owing to Dnmt5 inhibition from ATP depletion or SAH accumulation). Third, we tested whether Dnmt5 activity on unmethylated DNA substrates could be detected under multiple turnover conditions after reactions of longer duration (4 hr) and increased concentration of the methyl donor ^{3}H-SAM (8 μM). Tritium incorporation into the hemimethylated substrate was ~1,200-fold greater than background level, as assessed in a reaction containing substrate DNA and ^{3}H-SAM but no enzyme (Figure 1F). Tritium incorporation into the unmethylated substrate, however, was indistinguishable from background. Finally, we examined Dnmt5 under single-turnover conditions in the presence of mononucleosomal substrates designed to more faithfully mimic the chromatin context of in vivo Dnmt5 activity. We reconstituted mononucleosomes that were flanked on either side by 40 bp linker DNA containing two CG sites, which were either unmethylated or hemimethylated (Figure 1G). We also generated analogous mononucleosomes that were modified using methyl-lysine analog technology to contain a histone mark associated with heterochromatic sites of Dnmt5 activity in vivo (denoted H3Kc9me3). The dynamic range of DNA methylation in these nucleosomal assays was less than that observed in the aforementioned multiple-turnover assays with non-nucleosomal DNA substrates, but the qualitative results were equivalent. Namely, Dnmt5 was active on nucleosomal substrates containing hemimethylated DNA, but not on those containing unmethylated DNA. Furthermore, the H3Kc9me3 mark did not provoke Dnmt5 activity on unmethylated substrates (Figure 1G).

Dnmt5 ATPase activity is sensitive to DNA substrate methylation and is required for cytosine methylation

We next investigated the nature of ATP's requirement in DNA methylation by Dnmt5. When Dnmt5 was incubated with hemimethylated DNA, both Mg^{2+} and ATP were required for DNA methylation activity (Figure 2A). Dnmt5 was not active in the presence of ADP or any nucleotide analog tested, including non-hydrolyzable ATP analogs such as AMP-PNP (Figure 2B). Furthermore, AMP-PNP added to reactions containing Dnmt5 and ATP was able to compete with ATP and block DNA methylation (Figure S2A). These results suggested that ATP hydrolysis might be required for methyltransferase activity, a potential role for Dnmt5's SNF2 family domain. This domain belongs to a subfamily of RING finger-containing SNF2 domains, which are present in Rad5, Rad16, HLTF, and SHPRH (Flaus et al., 2006; Huff and Zilberman, 2014).

To test whether Dnmt5 hydrolyzes ATP, we performed an NADH-coupled ATPase assay using full-length Dnmt5. Dnmt5 exhibited a basal ATPase activity of approximately 1 min^{-1}, which was stimulated ~2-fold by saturating concentrations of unmethylated dsDNA (Figure 2C). We next tested whether methylated DNA would differentially stimulate ATPase activity. We incubated Dnmt5 with saturating concentrations of 60 bp dsDNA substrates whose three CG sites were uniformly unmethylated, methylated, or symmetrically methylated (Figure 2C). Hemimethylated DNA was most stimulatory (~9-fold), whereas symmetrically methylated DNA was intermediate (~4-fold) and unmethylated DNA least stimulatory (~2-fold). The efficacy with which unmethylated DNA substrates stimulated ATPase activity did not depend on the presence of the CG motif, and varied slightly as DNA length was altered (Figure S2B,C). In contrast, the efficacy of hemimethylated substrates did not vary with their number of CG sites or length, and was universally greater than that of unmethylated DNA (Figure S2D).

Using the same DNA substrates, we next measured the ATPase kinetic parameters ($K_m^{app,ATP}$ and k_{cat}^{ATPase}). The parameters differed as a function of the DNA substrate, with hemimethylated DNA effecting significantly greater $K_m^{app,ATP}$ (6.2 versus 0.9 μM) and k_{cat}^{ATPase} (11.1 versus 2.4 min^{-1}) than did unmethylated DNA (Figure 2C). These findings indicate that the methylation state of the DNA substrate bound to Dnmt5 promotes an altered conformation, and in turn activity, of its SNF2 domain's nucleotide-binding pocket.

To confirm the SNF2 domain's role in ATPase activity, we mutated a region expected to play a role in binding ATP: its Walker A motif (K1469A mutation; Figure 2D). In the presence of unmethylated DNA, the K1469A mutation increased $K_m^{app,ATP}$ but had no effect on k_{cat}^{ATPase}, as expected (Figure 2E). Surprisingly, the mutation had a different effect on ATPase activity in the setting of hemimethylated DNA, where no tested concentration of ATP could fully rescue Dnmt5(K1469A) ATPase activity (Figure 2F). This result suggests a unique conformation of the SNF2 domain in the presence of hemimethylated DNA, in which the K1469 residue plays an additional role beyond simply ATP binding. We reasoned that this additional role could involve coupling ATP hydrolysis to productive recognition of the hemimethylated substrate by the DNMT domain. We therefore tested the methyltransferase activity of Dnmt5(K1469A). Strikingly, Dnmt5(K1469A) showed no detectable methyltransferase activity even at a 1 mM ATP, a concentration at which its ATPase rate on hemimethylated substrates is readily detected (Figure 2F,G). Together, these results demonstrate that the SNF2 domain is responsive to DNA substrate methylation state, confirm that this domain is required for DNA methylation, and suggest that the K1469A mutation decouples ATPase activity from DNA methyltransferase activity.

Dnmt5 binds DNA substrates with a preference for hemimethylation, and its affinity is modulated by nucleotide binding

We next assessed DNA substrate binding by Dnmt5 in order to determine whether this function is regulated by the ATP hydrolysis cycle of the SNF2 domain. To establish a baseline for DNMT domain binding to DNA, we purified an MBP-fused, truncated form of Dnmt5 containing only the DNMT domain (residues 345–747) and assessed its ability to bind DNA using an electrophoretic mobility shift assay (EMSA) (Figure 3A). When

incubated with Cy5-labeled 60 bp DNA substrates equivalent to those used in the prior methyltransferase reactions, Dnmt5(345–747) bound unmethylated and hemimethylated DNA with similar affinity (K_d ~ 7 nM) (Figure 3B). Under the same conditions, DNA binding by an MBP-fused Dnmt5 truncation containing only the N-terminal chromodomain (residues 1–150) was not quantifiable, confirming that the MBP tag was not responsible for DNA binding (Figure S3A). DNA binding could be competed by excess concentrations of unlabeled DNA (Figure S3B). As expected, Dnmt5(345–747), which lacks the SNF2 domain, did not exhibit DNA methyltransferase activity (Figure S3C).

In order to test whether the Dnmt5 N- and C-terminal regions (peripheral to DNMT domain) influence DNA binding (Figure 3A), we performed EMSAs using full-length Dnmt5. Unlike Dnmt5(345–747), full-length Dnmt5 bound DNA differentially depending on methylation state (Figure 3C). The K_d of Dnmt5 for unmethylated and hemimethylated DNA was 20 ± 5 nM and <1 nM, respectively, the latter being an upper bound due to limitations of our assay. Dnmt5 binding to labeled DNA could be competed with excess concentrations of unmethylated or hemimethylated unlabeled DNA, confirming assay specificity (Figure S3D).

A simple interpretation of the above results is that the N- and/or C-terminal domains present in full-length Dnmt5 alter the DNMT domain's conformation so as to influence its affinity for DNA substrates. We hypothesized that the SNF2 domain plays such a role, and therefore tested whether manipulation of the SNF2 domain via nucleotides or nucleotide analogs would affect the ability of full-length Dnmt5 to bind hemimethylated DNA. Relative to the apo state, addition of ADP, ATP, AMP-PCP, and AMP-PNP reduced Dnmt5 affinity for hemimethylated DNA, with AMP-PNP having the largest effect (Figure 3D). We validated these effects by performing quantitative EMSA experiments (Figure 3E). Similar effects of nucleotides and analogs were observed in the context of Dnmt5 binding to unmethylated DNA (Figure S3E). Dissociation constants measured by EMSA in the presence of ATP were concordant with $K_m^{app,DNA}$ values for the same DNA substrates as measured by ATPase assay (Figure 3F). Importantly, nucleotides had no effect on DNA binding by Dnmt5(345–747), as expected because this truncation does not contain the SNF2 domain or its nucleotide-binding site (Figure S3F). These results indicate that the nucleotide-bound state of Dnmt5 influences its DNA binding ability, demonstrating a coupling between its SNF2 and DNMT domains.

Dnmt5 ATPase activity is responsive to CG base manipulations

The selective responsiveness of Dnmt5 ATPase activity to hemimethylated DNA suggested that ATPase activity is coupled to detection of optimal substrates for the methyltransferase activity of Dnmt5. We therefore sought to more specifically define the DNA features that stimulate ATPase activity, with a focus on the hemimethylated CG site itself.

We generated 60 bp dsDNA substrates that contain a single CG site, which was either unmethylated (CG/CG) or hemimethylated (mCG/CG) (Figure 4A). Each base in the mCG/CG motif, excepting the methylated cytosine, was then individually mutated to thymine (Figure 4B). To reduce the potential effects of mismatched bases, we also created a mutated substrate in which two alterations were made (mCA/TG). Each mutation of the

hemimethylated CG motif substantially reduced the its ability to stimulate ATPase activity, even with the substrates present at saturating concentrations (Figure 4C). Therefore, unlike unmethylated DNA, which stimulates ATPase activity to the same modest extent in the presence or absence of CG motifs (Figure S2C), hemimethylated DNA requires the intact CG motif for its full effect.

The sensitivity of ATPase activity to the CG motif is consistent with the idea that the SNF2 domain is coupled to hemimethylated CG detection by the DNMT domain, a protein fold able to make multiple contacts to a CG motif and to undergo activating conformational rearrangements when its preferred substrate is present (Matje et al., 2011; 2013; Song et al., 2012). Specifically, the paradigmatic cytosine methyltransferase M.HhaI has been found to follow a precatalytic pathway in which it 1) binds its DNA substrate, 2) destabilizes the target cytosine, causing it to flip out of the DNA helix, and 3) undergoes a conformational rearrangement to close its catalytic loop, creating a ‘closed’ active site capable of methylation (Matje et al., 2011; Roberts and Cheng, 1998; Sankpal and Rao, 2002). We hypothesized that these or analogous DNMT domain conformations in Dnmt5 may be coupled to its ATPase activity. Stabilizing such conformations would therefore be expected to activate the ATPase, bypassing its requirement for a hemimethylated substrate.

First, we tested the effect of SAM on Dnmt5 in the context of unmethylated DNA, since SAM is known to stabilize a flipped-cytosine conformation of M.HhaI bound to its DNA substrate (Klimasauskas et al., 1998). SAM addition had no effect on the ATPase activity of Dnmt5, however (Figure S4A). We next utilized a more potent approach by manipulating the strength of the hydrogen bonding potential of the target cytosine. Weakening this interaction by mutating the parental strand guanine increases the methylation activities of M.HhaI and DNMT1, presumably because it decreases the energetic cost of cytosine flipping and accelerates this step (Bashtrykov et al., 2012; Renbaum and Razin, 1995; Smith et al., 1991). This was not the case for Dnmt5, as mutation of one or both guanines in the unmethylated CG/CG motif did not increase ATPase activity (Figure S4B) or allow methyltransferase activity (Figure S4C). These results suggest the base-flipping mechanism employed by Dnmt5 may be rather distinct from those of M.HhaI and DNMT1.

Finally, we considered the possibility that our mutational analyses were confounded by the fact that we had manipulated the parental strand guanine, a residue that appeared to be particularly critical for stimulation of ATPase activity (Figure 4C). Indeed, targeted replacement of the parental strand guanine with an abasic site (in which the base is absent but the phosphate backbone and ribose ring remain) completely abrogated the ability of a hemimethylated substrate to stimulate ATPase activity and DNA methylation (abasic site indicated as ‘X’; Figure S4C,D). Thus, to avoid manipulating the parental strand guanine, we drew from extensive literature demonstrating that replacing the target cytosine itself with an abasic site increases DNMT domain affinity for its substrate while stabilizing the ‘closed’ catalytic loop conformation (Matje et al., 2011; 2013; O’Gara et al., 1998). These findings have been attributed to the fact that absence of the target cytosine obviates the energetic cost of base flipping.

We predicted that such an abasic substrate would bind with increased affinity to Dnmt5 and stabilize its DNMT domain in a ‘closed’ catalytic loop conformation analogous to the intermediate step of the cytosine methylation precatalytic pathway. We generated 60 bp unmethylated dsDNA substrates in which either the Watson or Crick strand target cytosine was replaced by an abasic site (Figure 4D). As assessed by EMSA, the abasic substrate bound full-length Dnmt5 with 5-fold greater affinity than did the unmethylated substrate, consistent with the idea that this substrate engages the DNMT domain (Figure 4E). We next tested the ability of saturating concentrations of abasic DNA substrates to induce SNF2 domain ATPase activity. Remarkably, each abasic substrate, despite lacking a methylation mark, stimulated ATPase activity to the same extent as did the hemimethylated CG substrate (Figure 4F). Finally, we measured k_{cat} and $K_m^{app,DNA}$ for each DNA substrate using an ATPase assay. The abasic substrate recapitulated the effects of the hemimethylated substrate: decreased $K_m^{app,DNA}$ and increased k_{cat}, as compared to unmethylated DNA (Figure 4G). These results implicate the DNMT domain and its precatalytic conformational changes as inputs to SNF2-mediated ATPase activity.

DISCUSSION

Our recent work indicates that Dnmt5 is an exceptionally specific maintenance methyltransferase both in vitro and in vivo. We therefore biochemically characterized its regulation, and found this enzyme to exhibit a novel DNA methylation mechanism in which its methyltransferase activity is coupled to the ATP hydrolysis activity of a SNF2 domain encoded on the same polypeptide. ATPase activity is responsive to hemimethylated CG motifs, and potentially regulated by DNMT domain conformational changes during the precatalytic pathway of DNA methylation. We discuss below the possibility that the coupling of DNMT activity to a seemingly needless expenditure of ATP enables increased Dnmt5 substrate specificity.

Dnmt5 is a cytosine methyltransferase with high specificity for hemimethylated DNA

The present findings extend our prior work demonstrating that Dnmt5 possesses extraordinary specificity for hemimethylated substrates. We detect no Dnmt5 in vitro methyltransferase activity on unmethylated CG sites in a variety of substrates, including nucleosomal substrates that mimic the H3K9me3-decorated heterochromatin at the in vivo regions of Dnmt5 activity. Using DNA methylation assays under multiple-turnover conditions, we estimate ~1,000-fold as a lower bound of Dnmt5’s preference for hemimethylated DNA, which is probably a substantial underestimate of the true value given that Dnmt5 activity slows over the reaction course (likely owing to ATP depletion and enzyme inhibition by the reaction product SAH). Dnmt5’s specificity does not appear to require processive action, since it is observed using substrates containing only a single hemimethylated CG site.

Importantly, we measured specificity in the context of saturating levels of DNA substrates, and it might be enhanced still further in vivo by Dnmt5’s binding affinity preference for hemimethylated DNA. The demonstrated recognition of H3K9 methylation by the Dnmt5 chromodomain could contribute additional specificity by favoring Dnmt5 localization at

heterochromatic regions enriched in hemimethylated CG sites, as could the previously demonstrated roles of Uhrf1 and Swi6 in the Dnmt5 methylation system (Catania et al., 2020). Although exact definitions of substrate specificity in DNA methyltransferases are challenging (Jeltsch, 2006), our observations indicate that Dnmt5 exhibits substantially more specificity than does the paradigmatic maintenance DNA methyltransferase DNMT1, which has a 20–40-fold preference for hemimethylated DNA in vitro. Dnmt5 therefore appears unusually well-equipped to faithfully maintain 5mC marks, in a purely epigenetic fashion, over long timescales (Catania et al., 2020; Jeltsch and Jurkowska, 2014).

Dnmt5 ATP hydrolysis is stimulated by hemimethylated substrates and necessary for methyltransferase activity

The Dnmt5 family of DNA methyltransferases is characterized by the presence of a SNF2 helicase-like domain (Iyer et al., 2011; Ponger and Li, 2005), but the role of this domain has not been investigated. Using nucleotide analogs and Dnmt5 mutagenesis, our present results demonstrate that SNF2-mediated ATP hydrolysis by Dnmt5 is strictly required for its DNA methyltransferase activity.

SNF2 homologs have long been implicated in DNA methylation. Lsh and DDM1 are required for DNA methylation in mouse and *Arabidopsis*, respectively (Dennis et al., 2001; Jeddeloh et al., 1999; Vongs et al., 1993). The role of these factors appears distinct from that of Dnmt5, however. Lsh and DDM1 are thought to remodel nucleosomes in order to overcome the nucleosome's inhibitory effect on DNA methylation (Brzeski and Jerzmanowski, 2003; Felle et al., 2011; Ren et al., 2015; Zemach et al., 2013). Indeed, the requirement for DDM1 in vivo can be suppressed by additional mutations (such as loss of histone H1) that impede nucleosome compaction (Zemach et al., 2013). In contrast, the Dnmt5 SNF2 domain is absolutely required for DNA methylation even in non-nucleosomal contexts. Furthermore, Dnmt5 belongs to a subfamily of SNF2 domains (with Rad5, HLTF, and SHPRH) that has not been associated with nucleosome remodeling activity (Huff and Zilberman, 2014; Unk et al., 2010), and it encodes alterations of several DNA-binding motifs (e.g., Ib, Ic, IIa, IVa) that are broadly conserved in bona fide SNF2 family chromatin remodelers (Data S1). What, then, is the purpose of ATP hydrolysis by Dnmt5, an expenditure of energy not fundamentally required for the transfer of a methyl group from SAM to cytosine?

Several lines of evidence suggest that the conformation the SNF2 ATPase of Dnmt5 is coupled to the detection of preferred DNA substrates by its DNMT domain. First, the catalytic parameters of SNF2-mediated ATP hydrolysis are significantly different in the presence of different DNA substrates. Specifically, the $K_m^{app,ATP}$ and k_{cat}^{ATPase} are higher in the presence of hemimethylated substrate than in the presence of unmethylated substrate. Second, a Walker A site mutation (K1469A) has different effects on SNF2 activity in the presence of hemimethylated versus unmethylated substrates. In the presence of unmethylated DNA, the effect of this mutation can be completely rescued by high concentrations of ATP, consistent with a role for K1469 solely in ATP binding. In contrast, in the presence of hemimethylated DNA, high ATP concentrations do not fully rescue SNF2 ATPase activity, and DNA methyltransferase activity is absent despite detectable ATPase

activity. Therefore, the K1469 residue, uniquely in the setting of hemimethylated substrate, appears to play an additional role, perhaps acting to couple ATP hydrolysis to productive DNA methylation. Third, nucleotide binding by the SNF2 domain impacts the affinity of the DNMT domain for DNA. Fourth, SNF2 ATPase activity can be stimulated by engineered abasic DNA substrates designed to specifically engage the DNMT domain and stabilize its active conformation.

Together, these results highlight an interdomain communication within Dnmt5 that is critically required for DNMT activity. Although structural information will ultimately be required to fully understand the basis of the coupling, a simple interpretation is that protein allostery plays a major role (as opposed to interdomain communication transmitted through conformational change of the DNA substrate itself). This conclusion is supported by our finding that very subtle manipulations of the mCG/CG target site are sufficient to modulate SNF2 ATPase activity throughout its full dynamic range (e.g., Figure 4C, S4D), whereas changes in DNA substrate length, sequence, and CG site number/location have minimal effect. Furthermore, a Dnmt5 fragment consisting of only the SNF2 domain does not exhibit DNA-stimulated ATP hydrolysis, nor does it bind DNA under conditions in which the DNMT domain readily does (Figure S4E–G). A second important question for future study is to more precisely define each aspect of DNMT domain conformational change—from cytosine flipping and pre-catalytic rearrangements to methyltransfer and product release—that stimulates (or requires) ATPase activity. Efforts have thus far been challenged by the high sensitivity of Dnmt5 to changes in the CG motif: methyltransferase activity is detectable only in the presence of the unaltered mCG/CG sequence (Figure S4C).

ATP hydrolysis as a means for cytosine methyltransferase specificity

Our observations are consistent with a model in which ATPase activity provides an opportunity for Dnmt5 to adopt an active conformation (E^a in Figure 4H) that is competent for DNA methylation. Several aspects of this model could contribute to Dnmt5's preference for maintenance DNA methylation. First, Dnmt5 binds substrates with a preference for hemimethylated versus unmethylated DNA. Second, analogous to the behavior of 'cognate' substrates in the well-studied M.HhaI system, hemimethylated DNA substrates may more readily enable conformational changes such as target cytosine flipping and DNMT domain activation loop closure, thereby leading to ATPase activity and adoption of the activated enzyme state E^a (Matje et al., 2013). In support of this idea, we find maximal rates of ATP hydrolysis in the presence of hemimethylated substrates, an effect that can be mimicked by abasic substrates designed to induce activating conformational changes of the DNMT domain. Third, after ATP hydrolysis, additional specificity may be provided by any chemical steps of DNA methylation or product release that themselves are sensitive to DNA substrate methylation state.

An additional potential mechanism of specificity is suggested by our observation that not every ATP hydrolysis event leads to productive DNA methylation. Specifically, we found that the increased ability of hemimethylated substrates to stimulate ATPase activity (~4-fold k_{cat}^{ATPase} difference versus unmethylated substrates) is not sufficient to explain the difference in DNA methyltransferase activity on these same two substrates (>1,000-fold).

Such a discordance would not be possible if every ATPase hydrolysis event were linked to a productive DNA methylation event. This result, taken together with our finding that AMP-PNP reduces Dnmt5's DNA affinity by >100-fold, raises the possibility of substrate ejection during the ATP hydrolysis cycle (Figure 4H). In such a model, ATP hydrolysis provides an extra, irreversible step between substrate binding and reaction completion. Dissociation of the enzyme-substrate complex during the hydrolysis cycle, if occurring preferentially for unmethylated substrates, would provide additional substrate specificity, since this discard step is thermodynamically driven out from the productive methylation pathway by virtue of ATP hydrolysis (Burgess and Guthrie, 1993; Hopfield, 1974; Ninio, 1975; Yarus, 1992a; 1992b). Our proposed model thus shares conceptual elements with classical models of kinetic proofreading.

Importantly, formal demonstration of a kinetic proofreading model for Dnmt5 awaits further kinetic studies as well as the development of substantially more sensitive assays that can measure the rate of DNA methylation on 'non-cognate' unmethylated DNA substrates. The latter is important for addressing to the possibility that a portion of the ATP hydrolysis we observe in the context of unmethylated DNA is not engaged in proofreading but rather 'off-pathway' and fundamentally incapable of promoting DNA methylation (Yarus, 1992a). Despite these caveats, we note that kinetic proofreading principles have been invoked for many other helicase-related enzymes, both inside and outside the SNF2 family (Narlikar, 2010; Staley and Guthrie, 1998).

For instance, the innate immune receptor RIG-I is a DEXD/H family RNA helicase whose specific recognition of blunt-ended 5′ppp dsRNA leads to its oligomerization and triggers the innate immune response (Brisse and Ly, 2019). Just as the Dnmt5 ATPase domain neighbors a DNMT domain with high affinity for a hemimethylated CG motif, the RIG-I ATPase domain neighbors a 'repressor domain' that has high affinity for the 5′ppp RNA end motif. Like we observe for Dnmt5, parts of the RIG-I ATP binding and hydrolysis cycle are associated with reduced affinity for its nucleic acid substrates, providing an opportunity for kinetic proofreading (Devarkar et al., 2018; Lässig et al., 2015; Louber et al., 2015; Rawling et al., 2015). In clear contrast to Dnmt5, however, there appears to be minimal conformational coupling between the neighboring domains in RIG-I. Specifically, RIG-I's ATPase activity is not selectively responsive to the presence of the 5′ppp motif (Rawling et al., 2014), nor does ATP binding by the helicase domain affect the repressor domain's affinity for 5′ppp (Devarkar et al., 2018). Instead of acting to regulate a neighboring domain, ATP hydrolysis by the RIG-I helicase appears important primarily for RNA binding and translocation by the helicase domain itself.

To our knowledge, Dnmt5 represents the first example of a reaction mechanism in which ATP hydrolysis is coupled to cytosine methylation. We find that the principal requirement of the Dnmt5 SNF2 domain is not nucleosome remodeling. Instead, we propose that ATP hydrolysis acts in concert with precatalytic events at the DNMT domain to provide an opportunity for increased substrate specificity. Admittedly, the idea that ATP hydrolysis contributes to DNMT substrate specificity (as opposed to only methyltransferase activity per se) is at present challenging to test directly owing to the complete lack of detectable DNMT activity upon ATP withdrawal or K1469A mutation. Surmounting this challenge will likely

require creation of more subtle Dnmt5 mutants based on atomic-resolution structures of Dnmt5 in its various states. Nevertheless, our model may help explain the remarkable ability of *C. neoformans* Dnmt5 to mediate epigenome evolution of million-year timescales in the absence of a de novo methyltransferase (Catania et al., 2020).

STAR METHODS

RESOURCE AVAILABILITY

Lead contact—Further information and requests for resources and reagents should be directed to and will be fulfilled by the Lead Contact, Hiten D. Madhani (hitenmadhani@gmail.com).

Materials Availability—All reagents generated in this study are available without restriction.

Data and Code Availability—No large-scale data or code was generated for this study.

EXPERIMENTAL MODEL AND SUBJECT DETAILS

Full-length Dnmt5 protein was purified from its host organism (*C. neoformans* strain H99) or after recombinant expression in *S. cerevisiae* strain JEL1. Fragments encoding the Dnmt5 DNA methyltransferase domain (345–747) or SNF2 domain (1400–2377) was expressed and purified from *E. coli* strain BL21(DE3).

METHOD DETAILS

Protein expression and purification—Protein constructs were purified from *E. coli*, *C. neoformans*, or *S. cerevisiae*. For the former, a codon-optimized DNA sequence encoding the DNA methyltransferase domain of *C. neoformans* Dnmt5 (residues 345–747) was cloned into the pMAL vector. The *E. coli* strain BL21(DE3) was transformed, grown to OD_{600} = 0.8 in 2x YT medium, then induced with 1 mM IPTG overnight at 18°C. Recombinant MBP-Dnmt5(345–747)-6xHis was purified using Ni-NTA agarose resin (Qiagen) and measured by A_{280} (ε = 139,790 cm^{-1} M^{-1}). Recombinant MBP-Dnmt5(1400–2377)-6xHis was expressed and purified as above, and measured by A_{280} (ε = 170,830 cm^{-1} M^{-1}).

Full-length Dnmt5 was purified from *C. neoformans* using a strain in which the endogenous *DNMT5* gene was tagged (2xFLAG) and its promoter replaced by a galactose-inducible promoter (pGAL7) (Catania et al., 2020). This strain was grown at 30°C to OD_{600} = 2.0 in 4 L YPAG medium (1% yeast extract, 2% Bacto-peptone, 2% galactose, 0.015% L-tryptophan, 0.004% adenine), at which point the cells were harvested, resuspended in TAP buffer (25 mM HEPES-KOH pH7.9, 0.1 mM EDTA, 0.5 mM EGTA, 2 mM $MgCl_2$, 20% glycerol, 0.1% Tween-20, 300 mM KCl, 1 mM DTT, 1x EDTA-free Complete protease inhibitor (CPI; Roche)), snap frozen, then lysed using a coffee grinder (3 min) and mortar and pestle (30 min). Lysate was resuspended in TAP buffer and centrifuged at 27,000 x *g* for 40 min at 4°C, after which it was incubated in batch format with anti-FLAG M2 affinity resin (Sigma) for 4 hr. The resin was washed three times with TAP buffer totaling 1 hr. Tagged protein was eluted by three washes at 4°C in FLAG elution buffer (25 mM HEPES-

KOH pH7.9, 2 mM $MgCl_2$, 20% glycerol, 300 mM KCl, 1 mM DTT, 1x CPI, 0.4 mg/ml 3xFLAG peptide (Sigma)) totaling 1 hr. The eluted protein was dialyzed against storage buffer (50 mM HEPES-KOH pH 7.9, 150 mM KCl, 10% glycerol, 2 mM β-mercaptoethanol) and then concentrated in a 100k MWCO centrifugal filter (Amicon). Protein concentration was determined by A_{280} (ε = 308,450 cm^{-1} M^{-1}).

For expression in *S. cerevisiae*, full-length *C. neoformans* cDNA encoding Dnmt5–10xHis was cloned into the 83ν vector (Li et al., 2009), and used to transform the *S. cerevisiae* strain JEL1 (Lindsley and Wang, 1993). Starter cultures were grown overnight in SC -his medium with 2% glucose, then used to inoculate 2 L cultures of YPGL medium (1x YEP, 1.7% lactic acid, 3% glycerol, 0.12% glucose, 0.15 mM adenine) to a starting OD_{600} of 0.03. After growth at 30°C to an OD_{600} of 1.0, expression was induced by addition of 2% galactose. After 6 hr of continued growth at 30°C, cells were harvested, washed once in 1x TBS (50 mM Tris-Cl pH 7.6, 150 mM NaCl), and snap frozen. Frozen cells were lysed in a ball mill (6× 3 min at 15 Hz), resuspended in Ni-NTA lysis buffer (50 mM NaH_2PO_4 pH 8, 300 mM NaCl, 10% glycerol, 10 mM imidazole, 2 mM β-mercaptoethanol, 0.02% NP40, 1x CPI), and centrifuged 20,000 x *g* for 30 min at 4°C. Lysate was bound to Ni-NTA resin in batch format for 2 hr at 4°C. The resin was washed in column format using 5 bed volumes Ni-NTA buffer followed by 10 bed volumes Ni-NTA wash buffer (same as Ni-NTA lysis buffer except 20 mM imidazole). Bound protein was eluted with 4 bed volumes Ni-NTA elution buffer (same as Ni-NTA lysis buffer except 300 mM imidazole and no NP40). Eluted protein was dialyzed against storage buffer and applied to a HiTrap Q HP anion exchange column (GE Life sciences) pre-equilibrated in buffer A (50 mM HEPES-KOH pH 7.9, 150 mM KCl, 10% glycerol, 2mM β-mercaptoethanol). Fractions were collected across a 150–1000 mM KCl gradient, and those containing Dnmt5 were pooled, concentrated, dialyzed against storage buffer, and frozen. Protein concentration was determined by A_{280} (ε = 308,450 cm^{-1} M^{-1}).

DNA methyltransferase assay—DNA oligonucleotide substrates were synthesized by IDT (Coralville, IA) (Table S1). In most cases, DNA methylation was performed in multiple turnover conditions by incubating 30 nM recombinant Dnmt5 in DNMT reaction buffer (50 mM Tris pH 8, 25 mM NaCl, 10% glycerol, and 2 mM DTT) with 5 μM DNA substrate. When indicated, ATP and $MgCl_2$ were added at 1 mM, and histone tail peptides were added at 5 μM. Reactions were initiated at 23°C by addition of 4 μM ^{3}H-SAM (Perkin Elmer). Aliquots were removed at indicated time points and quenched in a solution of 10 mM SAM in 10 mM H_2SO_4. The quenched solution was pipetted onto DE81 filter paper and air dried for 15 min. Filter papers were then washed three times in 200 mM ammonium bicarbonate (5 min each), once with water (5 min), then rinsed twice in ethanol and dried for 20 min. Filters were added to scintillation fluid (Bio-Safe NA, Research Products International Corp.) and ^{3}H was detected in an LS 6500 scintillation counter (Perkin Elmer).

Electrophoretic mobility shift assay—DNA oligonucleotides labeled with 5′ Cy5 were synthesized by IDT (Coralville, IA) (Table S1) and annealed in annealing buffer (20 mM Tris pH 8, 1 mM EDTA, 50 mM NaCl), after which they were purified by polyacrylamide gel electrophoresis. Recombinant Dnmt5 was incubated with labeled DNA

probe (1–3 nM in a solution of 16 mM HEPES-KOH pH7.9, 8% glycerol, 40 mM KCl, 0.02% NP40, 1.6 mM DTT) for 20 min at 23°C, and then resolved in a polyacrylamide gel (4.5% acrylamide:bis 29:1 (Bio-Rad), 1% glycerol, 1x TBE) at 4°C. Preparations of Dnmt5 from *C. neoformans* and *S. cerevisiae* were independently assessed to confirm similar substrate binding preferences. Reported K_d values were determined using Dnmt5 protein expressed from *C. neoformans*. To assess the effects of nucleotide analogs on DNA binding, the analogs were mixed with equal concentration $MgCl_2$ and then added to DNA binding reactions at a final concentration of 1 mM. Gels were imaged using a Typhoon 9400 Imager (Amersham) and densitometry was performed using ImageJ (Schneider et al., 2012).

Generation of nucleosome substrates—DNA for nucleosome substrates was generated by PCR and corresponded to the Widom 601 nucleosome positioning sequence (147 bp) flanked on either side by a 40 bp linker sequence. Linkers each contained two CG sites that were either hemimethylated or unmethylated as dictated by the use of PCR primers containing 5mC (Table S1); the Widom 601 sequence was entirely unmethylated. Amplified DNA was ethanol precipitated and resolved in a 5% acrylamide gel. A gel slice containing the product was cut out, sheared by passing through a syringe, then incubated in TE buffer overnight at 23°C with rocking to extract DNA; soluble DNA was purified by ethanol precipitation.

Mononucleosomes were assembled using purified reconstituted histone octamer generated with recombinant bacterially expressed histones from *Xenopus laevis.* For H3K9me3 nucleosomes, H3 histones were modified using methyl lysine analog (MLA) technology before reconstitution into octamer (Simon, 2010). Optimal ratios of DNA:octamer:dimer for nucleosome assembly were determined empirically by varying octamer:dimer in small-scale assembly reactions. Nucleosomes were reconstituted by salt dialysis over 36–48 hours, purified over 10–30% glycerol gradients using ultracentrifugation, and concentrated before use.

NADH-coupled ATPase assay—ATPase activity was assessed by incubating recombinant Dnmt5 (30–60 nM) in ATPase reaction buffer (50 mM HEPES-KOH pH 7.9, 75 mM KCl, 5% glycerol, 2 mM DTT, 2 mM phosphoenolpyruvate, 0.18 mM NADH, 0.5 mM ATP, 5 mM $MgCl_2$, 10 U/ml pyruvate kinase (Sigma), and 10 U/ml lactate dehydrogenase (EMD Millipore)). DNA substrates were added typically at 5 μM in 80 μl reactions in 384 well non-stick clear bottom plates (Corning 3655). Separate experiments with varying DNA concentration were performed to confirm that each substrate was present at saturating concentration. Preparations of Dnmt5 from *C. neoformans* and *S. cerevisiae* were independently assessed to confirm similar ATPase properties. Reactions were monitored in a Spectramax M5e plate reader (Molecular Devices) for absorbance at 340 nm and 420 nm over 30 min at 23°C. To assess rate, the difference between A340 and A420 was plotted versus time.

Protein domain identification and alignment—Identification of the Dnmt5 gene in *C. neoformans* was based on annotations of the *var. grubii* H99 genome by the Broad Institute (Cambridge, MA). Dnmt5 protein domains were identified using SMART (Schultz et al.,

1998), and its primary sequence was compared to related proteins using Clustal Omega (Sievers et al., 2011) (Data S1).

QUANTIFICATION AND STATISTICAL ANALYSIS

DNA methylation assays were generally performed in multiple turnover conditions, with background signal determined using reactions lacking Dnmt5 enzyme. Owing to noisiness at near-background signal levels, a reaction was considered to yield measurable signal only when its signal was >2-fold above background cpm at every time point. Serial dilution experiments verified that ^{3}H detection was linear to the background signal level. Background signal was typically 50–100 cpm, whereas signal for productive reactions ranged from ~1,000 to ~100,000. For productive reactions, rates were calculated over the first 15–20 min where reaction progress was linear and <10% of available hemimethylated sites had been acted upon. These rate values were divided by Dnmt5 concentration to obtain k_{obs}. Separate experiments with varying DNA concentration were performed to confirm that each DNA substrate was present at saturating concentration. Linear fit of rate data was performed using Prism 6 (Graphpad Software).

ATPase assays were generally performed under multiple turnover conditions, and the initial linear portion of the curve was fit to determine reaction rate using Prism 6 (GraphPad Software). Separate experiments with varying DNA concentration were performed to confirm that each DNA substrate was present at saturating concentration. For measurement of $K_m^{app,ATP}$ and $K_m^{app,DNA}$, ATP or DNA concentration was varied in the presence of saturating amounts of DNA or ATP, respectively, and plots of rate versus concentration were fitted to the Michaelis-Menten equation using Prism 6 (Graphpad Software).

For EMSA DNA-binding assays, dissociation constants were determined from plots of fraction probe bound versus Dnmt5 concentration by fitting the equation $Y = b + (m - b) * \frac{R + X + Kd - \sqrt{(R + X + Kd)^2 - (4 * R * X)}}{2R}$ using Prism 6 (GraphPad Software) (Pagano et al., 2011). In this equation, b represents base signal (0, for 0% probe bound), m represents maximum signal (100, for 100% probe bound), R represents labeled probe concentration, X represents protein concentration, and Y represents percent probe bound, which was determined by quantifying the level of unbound probe.

In all experiments, N value represents number of independently prepared reactions. N value for each experiment and error bar definitions are indicated in each Figure legend. ATPase and methyltransferase kinetic parameters were confirmed across multiple independent purified protein preparations.

Supplementary Material

Refer to Web version on PubMed Central for supplementary material.

ACKNOWLEDGEMENTS

We thank C. Chio, D. Elnatan, K. Kay, L. Pack, J. Reuter, K. Verba, and members of the Madhani and Narlikar laboratories for helpful discussions, and N. Nguyen for media preparation. This work was supported by the National Institutes of Health (H.D.M. and G.J.N.). H.D.M. is a Chan-Zuckerberg Biohub Investigator.

REFERENCES

Arand J, Spieler D, Karius T, Branco MR, Meilinger D, Meissner A, Jenuwein T, Xu G, Leonhardt H, Wolf V, et al. (2012). In vivo control of CpG and non-CpG DNA methylation by DNA methyltransferases. PLoS Genet 8, e1002750. [PubMed: 22761581]

Bashtrykov P, Ragozin S, and Jeltsch A (2012). Mechanistic details of the DNA recognition by the Dnmt1 DNA methyltransferase. FEBS Lett 586, 1821–1823. [PubMed: 22641038]

Brisse M, and Ly H (2019). Comparative Structure and Function Analysis of the RIG-I-Like Receptors: RIG-I and MDA5. Front Immunol 10, 1586. [PubMed: 31379819]

Brzeski J, and Jerzmanowski A (2003). Deficient in DNA methylation 1 (DDM1) defines a novel family of chromatin-remodeling factors. J Biol Chem 278, 823–828. [PubMed: 12403775]

Burgess SM, and Guthrie C (1993). Beat the clock: paradigms for NTPases in the maintenance of biological fidelity. Trends Biochem Sci 18, 381–384. [PubMed: 8256287]

Canzio D, Chang EY, Shankar S, Kuchenbecker KM, Simon MD, Madhani HD, Narlikar GJ, and Al-Sady B (2011). Chromodomain-mediated oligomerization of HP1 suggests a nucleosome-bridging mechanism for heterochromatin assembly. Mol Cell 41, 67–81. [PubMed: 21211724]

Catania S, Dumesic PA, Pimentel H, Nasif A, Stoddard CI, Burke JE, Diedrich JK, Cook S, Shea T, Geinger E, et al. (2020). Evolutionary Persistence of DNA Methylation for Millions of Years after Ancient Loss of a De Novo Methyltransferase. Cell 180, 263–277.e20. [PubMed: 31955845]

Dennis K, Fan T, Geiman T, Yan Q, and Muegge K (2001). Lsh, a member of the SNF2 family, is required for genome-wide methylation. Genes Dev 15, 2940–2944. [PubMed: 11711429]

Devarkar SC, Schweibenz B, Wang C, Marcotrigiano J, and Patel SS (2018). RIG-I Uses an ATPase-Powered Translocation-Throttling Mechanism for Kinetic Proofreading of RNAs and Oligomerization. Mol Cell 72, 355–368.e4. [PubMed: 30270105]

Dürr H, Körner C, Müller M, Hickmann V, and Hopfner K-P (2005). X-ray structures of the Sulfolobus solfataricus SWI2/SNF2 ATPase core and its complex with DNA. Cell 121, 363–373. [PubMed: 15882619]

Fairman-Williams ME, Guenther U-P, and Jankowsky E (2010). SF1 and SF2 helicases: family matters. Curr Opin Struct Biol 20, 313–324. [PubMed: 20456941]

Felle M, Hoffmeister H, Rothammer J, Fuchs A, Exler JH, and Längst G (2011). Nucleosomes protect DNA from DNA methylation in vivo and in vitro. Nucleic Acids Research 39, 6956–6969. [PubMed: 21622955]

Feng S, Cokus SJ, Zhang X, Chen P-Y, Bostick M, Goll MG, Hetzel J, Jain J, Strauss SH, Halpern ME, et al. (2010). Conservation and divergence of methylation patterning in plants and animals. Proc Natl Acad Sci USA 107, 8689–8694. [PubMed: 20395551]

Flaus A, Martin DMA, Barton GJ, and Owen-Hughes T (2006). Identification of multiple distinct Snf2 subfamilies with conserved structural motifs. Nucleic Acids Research 34, 2887–2905. [PubMed: 16738128]

Gerasimaitė R, Merkienė E, and Klimasauskas S (2011). Direct observation of cytosine flipping and covalent catalysis in a DNA methyltransferase. Nucleic Acids Research 39, 3771–3780. [PubMed: 21245034]

Holliday R, and Pugh JE (1975). DNA modification mechanisms and gene activity during development. Science 187, 226–232. [PubMed: 1111098]

Hopfield JJ (1974). Kinetic proofreading: a new mechanism for reducing errors in biosynthetic processes requiring high specificity. Proc Natl Acad Sci USA 71, 4135–4139. [PubMed: 4530290]

Huff JT, and Zilberman D (2014). Dnmt1-independent CG methylation contributes to nucleosome positioning in diverse eukaryotes. Cell 156, 1286–1297. [PubMed: 24630728]

Iyer LM, Abhiman S, and Aravind L (2011). Natural history of eukaryotic DNA methylation systems. Prog Mol Biol Transl Sci 101, 25–104. [PubMed: 21507349]

Jaenisch R, and Bird A (2003). Epigenetic regulation of gene expression: how the genome integrates intrinsic and environmental signals. Nat Genet 33 Suppl, 245–254. [PubMed: 12610534]

Jeddeloh JA, Stokes TL, and Richards EJ (1999). Maintenance of genomic methylation requires a SWI2/SNF2-like protein. Nat Genet 22, 94–97. [PubMed: 10319870]

Jeltsch A (2006). On the enzymatic properties of Dnmt1: specificity, processivity, mechanism of linear diffusion and allosteric regulation of the enzyme. Epigenetics : Official Journal of the DNA Methylation Society 1, 63–66.

Jeltsch A, and Jurkowska RZ (2014). New concepts in DNA methylation. Trends Biochem Sci 39, 310–318. [PubMed: 24947342]

Jeltsch A, and Jurkowska RZ (2016). Allosteric control of mammalian DNA methyltransferases - a new regulatory paradigm. Nucleic Acids Research 44, 8556–8575. [PubMed: 27521372]

Jones PA, and Liang G (2009). Rethinking how DNA methylation patterns are maintained. Nat Rev Genet 10, 805–811. [PubMed: 19789556]

Klimasauskas S, Szyperski T, Serva S, and Wüthrich K (1998). Dynamic modes of the flipped-out cytosine during HhaI methyltransferase-DNA interactions in solution. Embo J 17, 317–324. [PubMed: 9427765]

Law JA, and Jacobsen SE (2010). Establishing, maintaining and modifying DNA methylation patterns in plants and animals. Nat Rev Genet 11, 204–220. [PubMed: 20142834]

Li E, Beard C, and Jaenisch R (1993). Role for DNA methylation in genomic imprinting. Nature 366, 362–365. [PubMed: 8247133]

Li M, Hays FA, Roe-Zurz Z, Vuong L, Kelly L, Ho C-M, Robbins RM, Pieper U, O'Connell JD, Miercke LJW, et al. (2009). Selecting optimum eukaryotic integral membrane proteins for structure determination by rapid expression and solubilization screening. J. Mol. Biol. 385, 820–830. [PubMed: 19061901]

Lindsley JE, and Wang JC (1993). On the coupling between ATP usage and DNA transport by yeast DNA topoisomerase II. J Biol Chem 268, 8096–8104. [PubMed: 8385137]

Matje DM, Coughlin DF, Connolly BA, Dahlquist FW, and Reich NO (2011). Determinants of precatalytic conformational transitions in the DNA cytosine methyltransferase M.HhaI. Biochemistry 50, 1465–1473. [PubMed: 21229971]

Matje DM, Zhou H, Smith DA, Neely RK, Dryden DTF, Jones AC, Dahlquist FW, and Reich NO (2013). Enzyme-promoted base flipping controls DNA methylation fidelity. Biochemistry 52, 1677–1685. [PubMed: 23409782]

Narlikar GJ (2010). A proposal for kinetic proof reading by ISWI family chromatin remodeling motors. Curr Opin Chem Biol 14, 660–665. [PubMed: 20833099]

Ninio J (1975). Kinetic amplification of enzyme discrimination. Biochimie 57, 587–595. [PubMed: 1182215]

O'Gara M, Horton JR, Roberts RJ, and Cheng X (1998). Structures of HhaI methyltransferase complexed with substrates containing mismatches at the target base. Nat. Struct. Biol 5, 872–877. [PubMed: 9783745]

Pagano JM, Clingman CC, and Ryder SP (2011). Quantitative approaches to monitor protein-nucleic acid interactions using fluorescent probes. Rna 17, 14–20. [PubMed: 21098142]

Ponger L, and Li W-H (2005). Evolutionary diversification of DNA methyltransferases in eukaryotic genomes. Mol Biol Evol 22, 1119–1128. [PubMed: 15689527]

Pradhan S, Bacolla A, Wells RD, and Roberts RJ (1999). Recombinant human DNA (cytosine-5) methyltransferase. I. Expression, purification, and comparison of de novo and maintenance methylation. J Biol Chem 274, 33002–33010. [PubMed: 10551868]

Rawling DC, Kohlway AS, Luo D, Ding SC, and Pyle AM (2014). The RIG-I ATPase core has evolved a functional requirement for allosteric stabilization by the Pincer domain. Nucleic Acids Research 42, 11601–11611. [PubMed: 25217590]

Ren J, Briones V, Barbour S, Yu W, Han Y, Terashima M, and Muegge K (2015). The ATP binding site of the chromatin remodeling homolog Lsh is required for nucleosome density and de novo DNA methylation at repeat sequences. Nucleic Acids Research 43, 1444–1455. [PubMed: 25578963]

Renbaum P, and Razin A (1995). Interaction of M.SssI and M.HhaI with single-base mismatched oligodeoxynucleotide duplexes. Gene 157, 177–179. [PubMed: 7607487]

Riggs AD (1975). X inactivation, differentiation, and DNA methylation. Cytogenet. Cell Genet 14, 9–25. [PubMed: 1093816]

Riggs AD, and Xiong Z (2004). Methylation and epigenetic fidelity. Proc Natl Acad Sci USA 101, 4–5. [PubMed: 14695893]

Roberts RJ, and Cheng X (1998). Base flipping. Annu Rev Biochem 67, 181–198. [PubMed: 9759487]

Sankpal UT, and Rao DN (2002). Structure, function, and mechanism of HhaI DNA methyltransferases. Crit. Rev. Biochem. Mol. Biol 37, 167–197. [PubMed: 12139442]

Schneider CA, Rasband WS, and Eliceiri KW (2012). NIH Image to ImageJ: 25 years of image analysis. Nat Methods 9, 671–675. [PubMed: 22930834]

Schultz J, Milpetz F, Bork P, and Ponting CP (1998). SMART, a simple modular architecture research tool: identification of signaling domains. Proc Natl Acad Sci USA 95, 5857–5864. [PubMed: 9600884]

Schübeler D (2015). Function and information content of DNA methylation. Nature 517, 321–326. [PubMed: 25592537]

Sievers F, Wilm A, Dineen D, Gibson TJ, Karplus K, Li W, Lopez R, McWilliam H, Remmert M, Söding J, et al. (2011). Fast, scalable generation of high-quality protein multiple sequence alignments using Clustal Omega. Mol. Syst. Biol 7, 539. [PubMed: 21988835]

Simon MD (2010). Installation of site-specific methylation into histones using methyl lysine analogs. Curr Protoc Mol Biol Chapter 21, Unit21.18.1–Unit21.18.10.

Smith SS, Kan JL, Baker DJ, Kaplan BE, and Dembek P (1991). Recognition of unusual DNA structures by human DNA (cytosine-5)methyltransferase. J. Mol. Biol 217, 39–51. [PubMed: 1988679]

Smith ZD, and Meissner A (2013). DNA methylation: roles in mammalian development. Nat Rev Genet 14, 204–220. [PubMed: 23400093]

Song J, Teplova M, Ishibe-Murakami S, and Patel DJ (2012). Structure-based mechanistic insights into DNMT1-mediated maintenance DNA methylation. Science 335, 709–712. [PubMed: 22323818]

Staley JP, and Guthrie C (1998). Mechanical devices of the spliceosome: motors, clocks, springs, and things. Cell 92, 315–326. [PubMed: 9476892]

Suzuki MM, and Bird A (2008). DNA methylation landscapes: provocative insights from epigenomics. Nat Rev Genet 9, 465–476. [PubMed: 18463664]

Tollefsbol TO, and Hutchison CA (1997). Control of methylation spreading in synthetic DNA sequences by the murine DNA methyltransferase. J. Mol. Biol 269, 494–504. [PubMed: 9217255]

Unk I, Hajdú I, Blastyák A, and Haracska L (2010). Role of yeast Rad5 and its human orthologs, HLTF and SHPRH in DNA damage tolerance. DNA Repair (Amst.) 9, 257–267. [PubMed: 20096653]

Velasco G, Hubé F, Rollin J, Neuillet D, Philippe C, Bouzinba-Segard H, Galvani A, Viegas-Péquignot E, and Francastel C (2010). Dnmt3b recruitment through E2F6 transcriptional repressor mediates germ-line gene silencing in murine somatic tissues. Proc Natl Acad Sci USA 107, 9281–9286. [PubMed: 20439742]

Vongs A, Kakutani T, Martienssen RA, and Richards EJ (1993). Arabidopsis thaliana DNA methylation mutants. Science 260, 1926–1928. [PubMed: 8316832]

Yarus M (1992a). Proofreading, NTPases and translation: constraints on accurate biochemistry. Trends Biochem Sci 17, 130–133. [PubMed: 1316651]

Yarus M (1992b). Proofreading, NTPases and translation: successful increase in specificity. Trends Biochem Sci 17, 171–174. [PubMed: 1317614]

Zemach A, Kim MY, Hsieh P-H, Coleman-Derr D, Eshed-Williams L, Thao K, Harmer SL, and Zilberman D (2013). The Arabidopsis nucleosome remodeler DDM1 allows DNA methyltransferases to access H1-containing heterochromatin. Cell 153, 193–205. [PubMed: 23540698]

Zemach A, McDaniel IE, Silva P, and Zilberman D (2010). Genome-wide evolutionary analysis of eukaryotic DNA methylation. Science 328, 916–919. [PubMed: 20395474]

HIGHLIGHTS

- Maintenance DNA methylation by Dnmt5 requires ATP hydrolysis by its SNF2 domain
- Hemimethylated DNA substrates preferentially stimulate Dnmt5 ATPase
- Mutation of Dnmt5 SNF2 domain decouples ATPase from DNA methyltransferase activity
- Stabilization of active DNMT domain conformation stimulates SNF2 ATPase

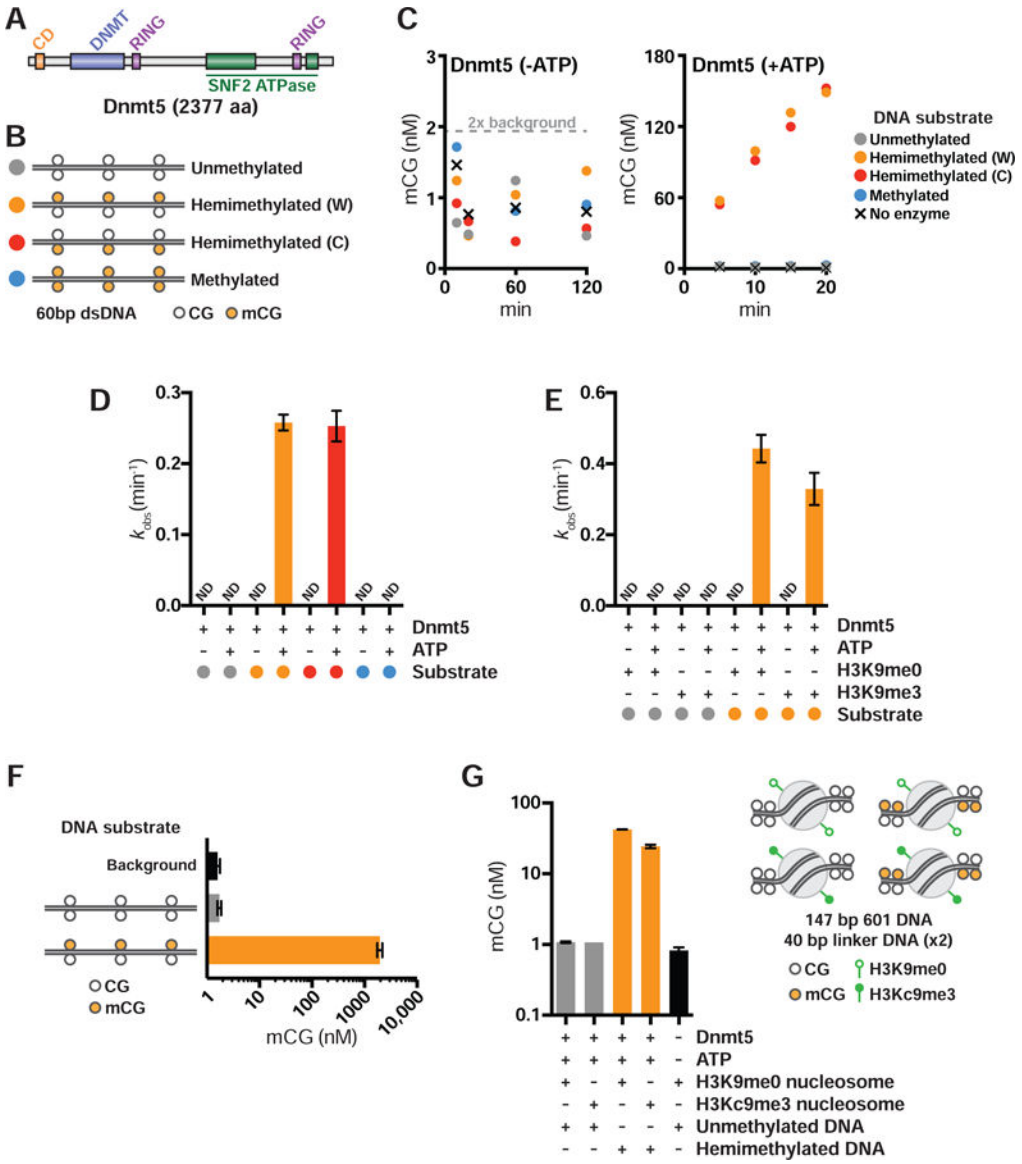

Figure 1. Dnmt5 is an ATP-dependent DNA methyltransferase with high specificity for hemimethylated substrates

(A) Protein domains in *C. neoformans* Dnmt5. **(B)** dsDNA substrates used in methyltransferase experiments. Each 60bp substrate contains three CG sites that are uniformly unmethylated, hemimethylated, or symmetrically methylated. **(C)** Example DNA methylation kinetics using 30 nM Dnmt5 and 5 μM each of the DNA substrates in B, with or without 1 mM ATP. **(D)** Average initial rates of Dnmt5 DNMT activity, in the presence or absence of 1 mM ATP. ND: no detectable activity; error represents SD; n = 4–5. **(E)** Average initial rates of Dnmt5 DNMT activity, in the presence or absence of 1 mM ATP and 5 μM histone tail peptides H3K9me0 or H3K9me3. ND: no detectable activity; error represent SD; n = 2–4. **(F)** DNMT activity of Dnmt5 (100 nM) on DNA substrates (5 μM) that were either unmethylated or hemimethylated. Measurement taken at 4 hr timepoint when reaction had ceased to progress. Background signal was measured in a reaction with unmethylated DNA but no enzyme. Graph represents average and SD; n = 3. **(G)** DNMT activity of Dnmt5 (150

nM) on nucleosomal substrates (50 nM). Measurement taken at 4 hr timepoint when reaction had ceased to progress. For each substrate, DNA is 227 bp sequence composed of Widom 601 nucleosome positioning sequence flanked by a 40 bp linker sequences. Linkers each contain two CG sites that are either hemimethylated or unmethylated; the Widom 601 sequence is entirely unmethylated. Nucleosomes are either wild-type (H3K9me0) or MLA (H3Kc9me3). Graph represents average and SD; n = 4. See also Figure S1.

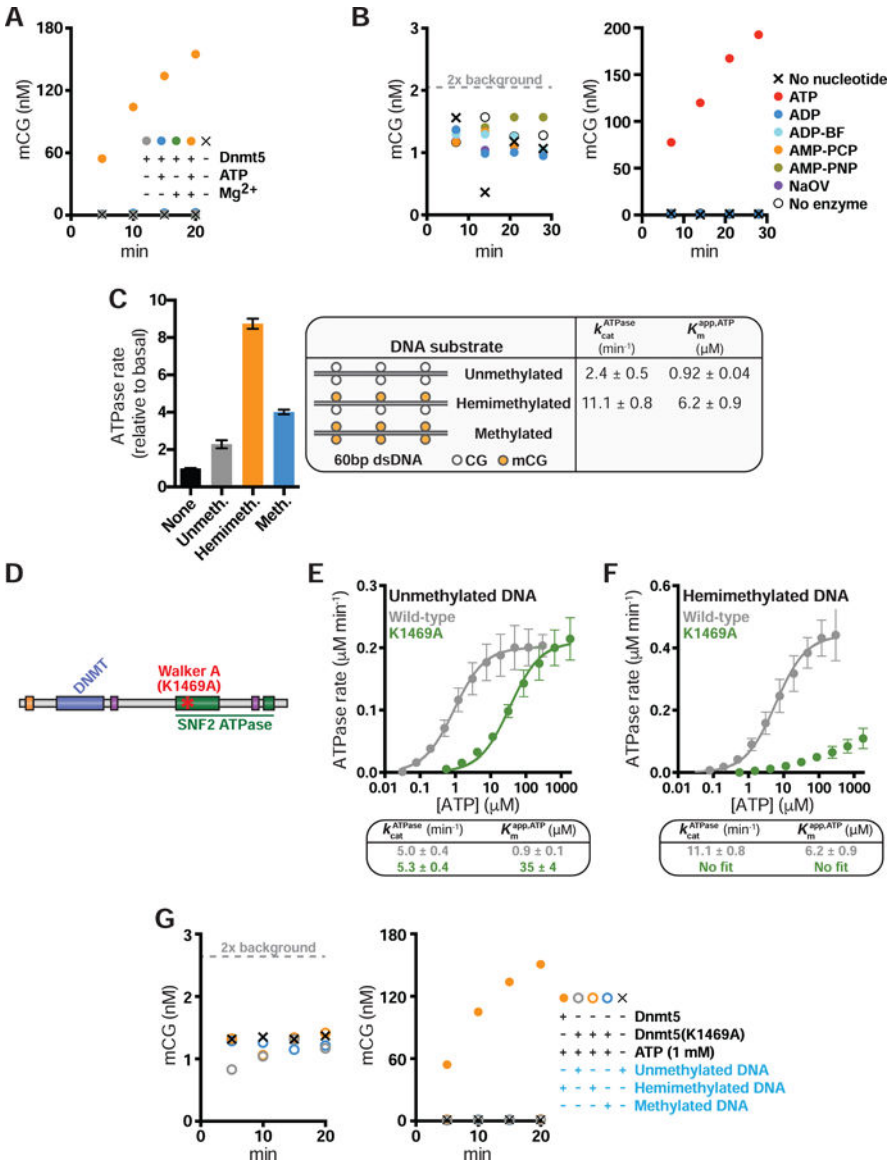

Figure 2. SNF2-mediated ATPase activity by Dnmt5 is sensitive to DNA substrate methylation and is required for DNA methyltransferase activity

(A) Example DNA methylation kinetics using 30 nM Dnmt5 and 5 μM hemimethylated DNA substrate, in the presence or absence of Mg^{2+} and ATP (1 mM). **(B)** Example DNA methylation kinetics using 30 nM Dnmt5 and 5 μM hemimethylated DNA substrate, in the presence of 1 mM nucleotide or analog: ATP, ADP, ADP beryllium fluoride (ADP-BF), AMP-PCP, AMP-PNP, sodium orthovanadate (NaOV). **(C)** Left: Average rates of ATPase activity in the presence of 40 nM Dnmt5 and 5 μM of the DNA substrates pictured. Data are normalized to ATPase rate in absence of DNA (1 min^{-1}). Error represents SD; n = 4. Right: Kinetic parameters of Dnmt5 ATPase activity measured in the presence of saturating amounts of unmethylated or hemimethylated DNA. Error represents SE; n = 2–4. **(D)** Mutation of a putative ATP-binding residue in Dnmt5. **(E-F)** Initial ATPase rates of 40 nM Dnmt5 or Dnmt5(K1469A) were determined at varying ATP concentrations in the presence of fixed, saturating concentrations of 80 bp unmethylated (E) or 60 bp hemimethylated (F)

DNA substrates. Error represents SD (graph) and SE (kinetic parameters); n = 4. **(G)** Example DNA methylation kinetics using 30 nM Dnmt5 or Dnmt5(K1469A) and 5 μM of the DNA substrates described in (C). See also Figure S2.

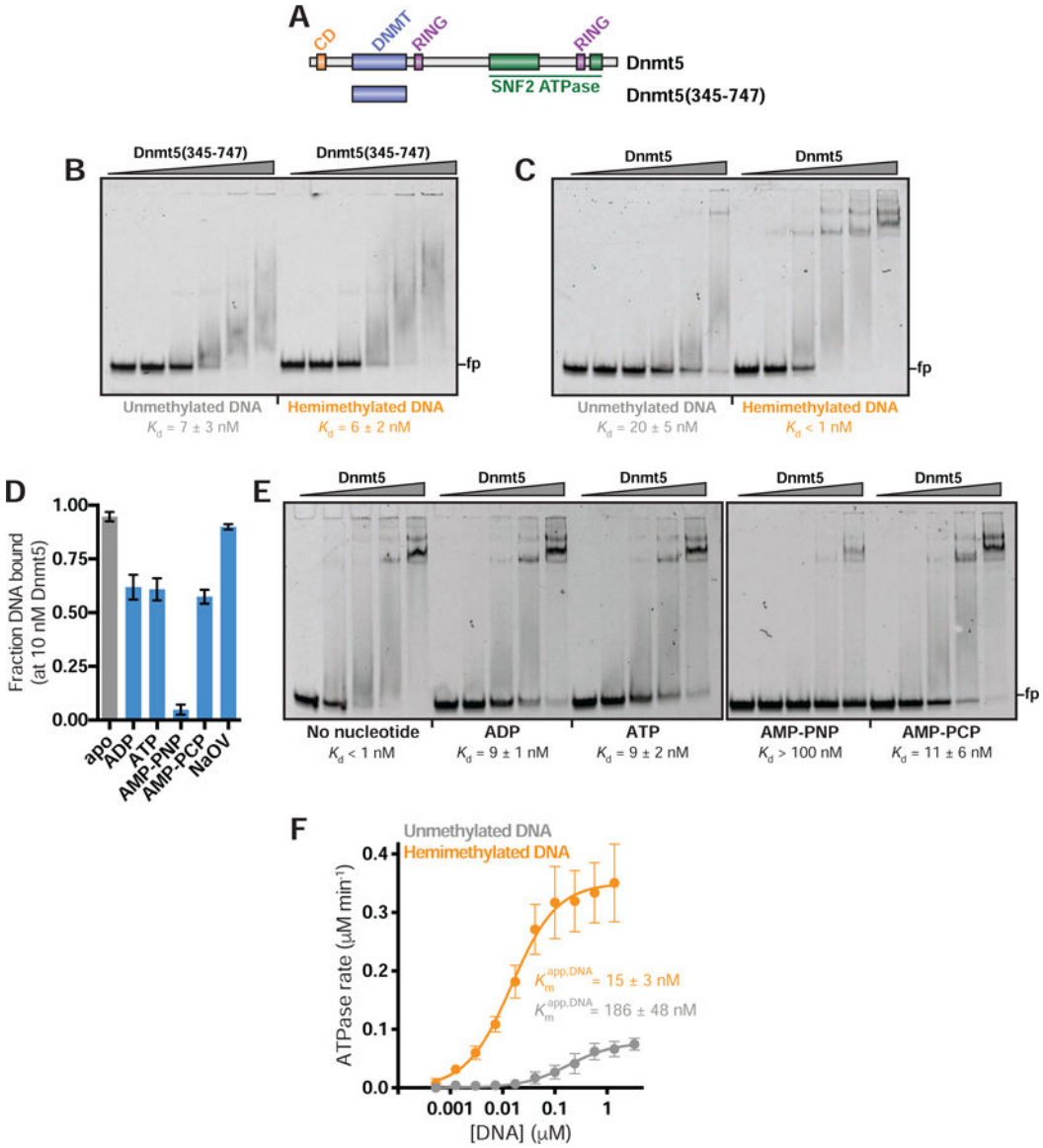

Figure 3. Nucleotide binding modulates the DNA affinity of Dnmt5

(A) Schematic illustrating the Dnmt5(345–747) truncation. **(B-C)** EMSA assessing binding of 0–67 nM Dnmt5(345–747) (B) or full-length Dnmt5 (C) to 1 nM labeled unmethylated or hemimethylated 60 bp dsDNA, using the same DNA substrates described in Figure 1B. K_d values represent average and SD; n=3–5. **(D)** Screen of nucleotide analogs for effects on Dnmt5 DNA binding. Dnmt5 (10 nM) was incubated with labeled hemimethylated DNA in the presence of nucleotide or analog (1 mM), and fraction probe bound was measured by EMSA. Graph represents average and SD; n = 4. **(E)** EMSA assessing binding of 0–50 nM full-length Dnmt5 to 1 nM labeled hemimethylated DNA in the presence of nucleotide or analog (1 mM). K_d values represent average and SD; n = 3. **(F)** Initial ATPase rates of 30 nM Dnmt5 were determined at varying concentrations of unmethylated or hemimethylated DNA substrates in the presence of fixed, saturating concentrations of ATP. Error represents SD (graph) and SE ($K_m^{app,DNA}$); n = 3. See also Figure S3.

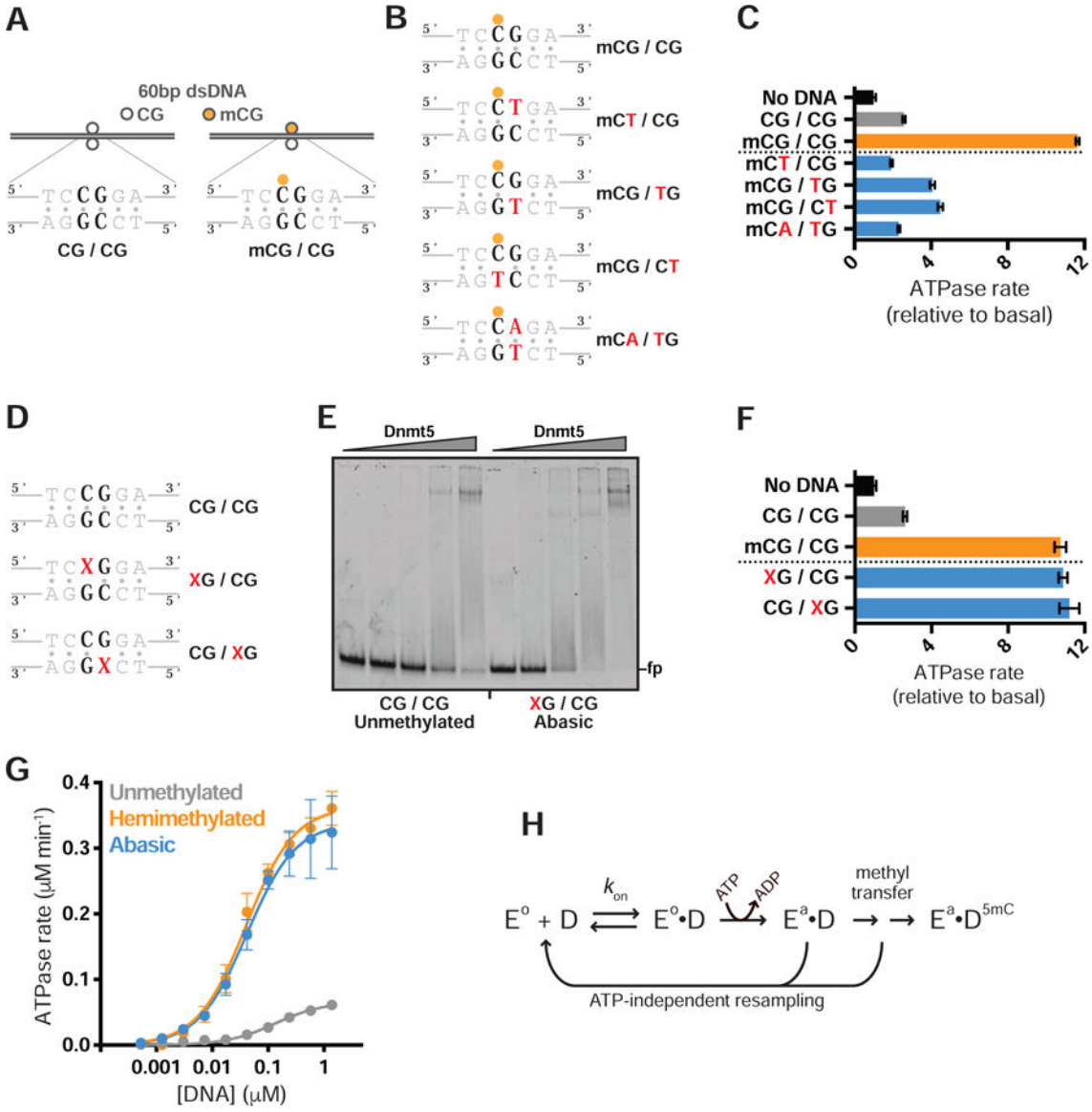

Figure 4. Dnmt5 ATPase activity is stimulated by DNA substrates predicted to stabilize intermediate steps of the cytosine methylation precatalytic pathway

(A) DNA substrates to assess effects of CG site manipulation. Each 60bp dsDNA substrate contains one CG site that is either unmethylated or hemimethylated. **(B)** Schematics of CG site mutant hemimethylated DNA substrates. Red color indicates base mutation. **(C)** Average rates of ATPase activity in the presence of 40 nM Dnmt5 and 5 μM of the DNA substrates described in panels A and B. Data are normalized to ATPase rate in absence of DNA (1 min^{-1}). Error represents SD; n = 4. **(D)** Schematics of abasic DNA substrates. Red color indicates base mutation. 'X' indicates abasic site. **(E)** EMSA assessing binding of full-length Dnmt5 (0–67 nM) to 1 nM labeled unmethylated or abasic site DNA. **(F)** Average rates of ATPase activity in the presence of 40 nM Dnmt5 and 5 μM of the DNA substrates described in panels A and D. Data are normalized to ATPase rate in absence of DNA (1 min^{-1}). Error represents SD; n = 3–4. **(G)** Initial ATPase rates of 30 nM Dnmt5 or Dnmt5(K1469A) were determined at varying concentrations of DNA substrate (unmethylated, hemimethylated, or

abasic site) in the presence of fixed, saturating concentrations of ATP. Error represents SD; n = 3. **(H)** Hypothetical model of ATPase stimulation by an intermediate step in the cytosine methylation precatalytic pathway. The inactive Dnmt5 enzyme (E^o) binds DNA (D), leading to conformational changes that include cytosine flipping and activation loop closure. The resulting E•D complex is competent for ATPase activity, resulting in an increased population of E^a, an active enzyme capable of DNA methylation. Each forward step may be sensitive to the methylation state of the DNA substrate, conferring selectivity for maintenance DNA methylation. ATP-independent resampling may also confer selectivity via mechanisms related to kinetic proofreading. See Discussion for details. See also Figure S4.

KEY RESOURCES TABLE

REAGENT or RESOURCE	SOURCE	IDENTIFIER
Antibodies		
Bacterial and Virus Strains		
E. coli BL21 (DE3) pLysS	Promega	Cat#L1195
Biological Samples		
Chemicals, Peptides, and Recombinant Proteins		
3xFLAG peptide	Millipore-Sigma	Cat#F4799
H3K9me0 peptide (ARTKQTARKSTGGKA)	Peptide 2.0	N/A
H3K9me3 peptide (ARTKQTARKme3STGGKA)	Peptide 2.0	N/A
H3K9me0 nucleosome (unmethylated DNA)	This study	N/A
H3K9me0 nucleosome (hemimethylated DNA)	This study	N/A
H3Kc9me3 nucleosome (unmethylated DNA)	This study	N/A
H3Kc9me3 nucleosome (hemimethylated DNA)	This study	N/A
(2-bromoethyl)-trimethylammonium bromide	Aldrich	Cat#117196
S-[methyl-^{3}H]-adenosyl-L-methionine	Perkin Elmer	Cat#NET155H250UC
Critical Commercial Assays		
Deposited Data		

REAGENT or RESOURCE	SOURCE	IDENTIFIER
Experimental Models: Cell Lines		
Experimental Models: Organisms/Strains		
C. neoformans NeoR-pGAL7–2xFLAG-Dnmt5	Catania et al., 2020	CM1844
S. cerevisiae JEL1 (α leu2 trip1 ura3–52 prb1–1122 pep4 Δhis3::PGAL1-GAL4)	Lindsley and Wang, 1993	N/A
Oligonucleotides		
DNA substrates	This paper	Table S1
Recombinant DNA		
83ν-Dnmt5–10xHis	Catania et al., 2020	BHM2244
83ν-Dnmt5(K1469A)-10xHis	This study	BHM2251
pMAL-Dnmt5(345–747)	This study	BHM2250
pMAL-Dnmt5(1400–2377)	This study	BHM2290
pMAL-Dnmt5(1–150-W87A, Y90A)	Catania et al., 2020	BHM2192
Pet3a-H2A (*Xenopus laevis*)	Canzio et al., 2011	N/A
Pet3a-H2B (*Xenopus laevis*)	Canzio et al., 2011	N/A
Pet3a-H3 (*Xenopus laevis*)	Canzio et al., 2011	N/A
Pet3a-H3-K9C (*Xenopus laevis*)	Canzio et al., 2011	N/A
Pet3a-H4 (*Xenopus laevis*)	Canzio et al., 2011	N/A
Software and Algorithms		
Prism 6	Graphpad	N/A

REAGENT or RESOURCE	SOURCE	IDENTIFIER
Other		

TABLE WITH EXAMPLES FOR AUTHOR REFERENCE

REAGENT or RESOURCE	**SOURCE**	**IDENTIFIER**
Antibodies		
Rabbit monoclonal anti-Snail	Cell Signaling Technology	Cat#3879S; RRID: AB_2255011
Mouse monoclonal anti-Tubulin (clone DM1A)	Sigma-Aldrich	Cat#T9026; RRID: AB_477593
Rabbit polyclonal anti-BMAL1	This paper	N/A
Bacterial and Virus Strains		
pAAV-hSyn-DIO-hM3D(Gq)-mCherry	Krashes et al., 2011	Addgene AAV5; 44361-AAV5
AAV5-EF1a-DIO-hChR2(H134R)-EYFP	Hope Center Viral Vectors Core	N/A
Cowpox virus Brighton Red	BEI Resources	NR-88
Zika-SMGC-1, GENBANK: KX266255	Isolated from patient (Wang et al., 2016)	N/A
Staphylococcus aureus	ATCC	ATCC 29213
Streptococcus pyogenes: M1 serotype strain: strain SF370; M1 GAS	ATCC	ATCC 700294
Biological Samples		
Healthy adult BA9 brain tissue	University of Maryland Brain & Tissue Bank; http://medschool.umaryland.edu/btbank/	Cat#UMB1455
Human hippocampal brain blocks	New York Brain Bank	http://nybb.hs.columbia.edu/
Patient-derived xenografts (PDX)	Children's Oncology Group Cell Culture and Xenograft Repository	http://cogcell.org/
Chemicals, Peptides, and Recombinant Proteins		
MK-2206 AKT inhibitor	Selleck Chemicals	S1078; CAS: 1032350–13-2
SB-505124	Sigma-Aldrich	S4696; CAS: 694433–59-5 (free base)
Picrotoxin	Sigma-Aldrich	P1675; CAS: 124–87-8
Human TGF-β	R&D	240-B; GenPept: P01137
Activated S6K1	Millipore	Cat#14–486
GST-BMAL1	Novus	Cat#H00000406-P01
Critical Commercial Assays		
EasyTag EXPRESS 35S Protein Labeling Kit	Perkin-Elmer	NEG772014MC
CaspaseGlo 3/7	Promega	G8090
TruSeq ChIP Sample Prep Kit	Illumina	IP-202–1012
Deposited Data		
Raw and analyzed data	This paper	GEO: GSE63473
B-RAF RBD (apo) structure	This paper	PDB: 5J17

REAGENT or RESOURCE	SOURCE	IDENTIFIER
Human reference genome NCBI build 37, GRCh37	Genome Reference Consortium	http://www.ncbi.nlm.nih.gov/projects/genome/assembly/grc/human/
Nanog STILT inference	This paper; Mendeley Data	http://dx.doi.org/10.17632/wx6s4mj7s8.2
Affinity-based mass spectrometry performed with 57 genes	This paper; and Mendeley Data	Table S8; http://dx.doi.org/10.17632/5hvpvspw82.1
Experimental Models: Cell Lines		
Hamster: CHO cells	ATCC	CRL-11268
D. melanogaster: Cell line S2: S2-DRSC	Laboratory of Norbert Perrimon	FlyBase: FBtc0000181
Human: Passage 40 H9 ES cells	MSKCC stem cell core facility	N/A
Human: HUES 8 hESC line (NIH approval number NIHhESC-09–0021)	HSCI iPS Core	hES Cell Line: HUES-8
Experimental Models: Organisms/Strains		
C. elegans: Strain BC4011: srl-1(s2500) II; dpy-18(e364) III; unc-46(e177)rol-3(s1040) V.	Caenorhabditis Genetics Center	WB Strain: BC4011; WormBase: WBVar00241916
D. melanogaster: RNAi of Sxl: y[1] sc[*] v[1]; P{TRiP.HMS00609}attP2	Bloomington Drosophila Stock Center	BDSC:34393; FlyBase: FBtp0064874
S. cerevisiae: Strain background: W303	ATCC	ATTC: 208353
Mouse: R6/2: B6CBA-Tg(HDexon1)62Gpb/3J	The Jackson Laboratory	JAX: 006494
Mouse: OXTRfl/fl: B6.129(SJL)-Oxtr$^{tm1.1Wsy}$/J	The Jackson Laboratory	RRID: IMSR_JAX:008471
Zebrafish: Tg(Shha:GFP)t10: t10Tg	Neumann and Nuesslein-Volhard, 2000	ZFIN: ZDB-GENO-060207–1
Arabidopsis: 35S::PIF4-YFP, BZR1-CFP	Wang et al., 2012	N/A
Arabidopsis: JYB1021.2: pS24(AT5G58010)::cS24:GFP(-G):NOS #1	NASC	NASC ID: N70450
Oligonucleotides		
siRNA targeting sequence: PIP5K I alpha #1: ACACAGUACUCAGUUGAUA	This paper	N/A
Primers for XX, see Table SX	This paper	N/A
Primer: GFP/YFP/CFP Forward: GCACGACTTCTTCAAGTCCGCCATGCC	This paper	N/A
Morpholino: MO-pax2a GGTCTGCTTTGCAGTGAATATCCAT	Gene Tools	ZFIN: ZDB-MRPHLNO-061106–5
ACTB (hs01060665_g1)	Life Technologies	Cat#4331182
RNA sequence: hnRNPA1_ligand: UAGGGACUUAGGGUUCUCUCUAGGGACUUAGGGUUCUCUCUAGGGA	This paper	N/A
Recombinant DNA		
pLVX-Tight-Puro (TetOn)	Clonetech	Cat#632162
Plasmid: GFP-Nito	This paper	N/A
cDNA GH111110	Drosophila Genomics Resource Center	DGRC:5666; FlyBase:FBcl0130415
AAV2/1-hsyn-GCaMP6- WPRE	Chen et al., 2013	N/A
Mouse raptor: pLKO mouse shRNA 1 raptor	Thoreen et al., 2009	Addgene Plasmid #21339
Software and Algorithms		

REAGENT or RESOURCE	SOURCE	IDENTIFIER
ImageJ	Schneider et al., 2012	https://imagej.nih.gov/ij/
Bowtie2	Langmead and Salzberg, 2012	http://bowtie-bio.sourceforge.net/bowtie2/index.shtml
Samtools	Li et al., 2009	http://samtools.sourceforge.net/
Weighted Maximal Information Component Analysis v0.9	Rau et al., 2013	https://github.com/ChristophRau/wMICA
ICS algorithm	This paper; Mendeley Data	http://dx.doi.org/10.17632/5hvpvspw82.1
Other		
Sequence data, analyses, and resources related to the ultra-deep sequencing of the AML31 tumor, relapse, and matched normal.	This paper	http://aml31.genome.wustl.edu
Resource website for the AML31 publication	This paper	https://github.com/chrisamiller/aml31SuppSite